First Direct Observation of a Nearly Ideal Graphene Band Structure

M. Sprinkle,[1] D. Siegel,[2] Y. Hu,[1] J. Hicks,[1] A. Tejeda,[3,4] A. Taleb-Ibrahimi,[5] P. Le Fèvre,[4] F. Bertran,[4] S. Vizzini,[6,7] H. Enriquez,[6,7] S. Chiang,[6,8] P. Soukiassian,[6,7] C. Berger,[1,9] W. A. de Heer,[1] A. Lanzara,[2] and E. H. Conrad[1]

[1]*The Georgia Institute of Technology, Atlanta, Georgia 30332-0430, USA*
[2]*Department of Physics, University of California, Berkeley, California 94720, USA and Advanced Light Source, Lawrence Berkeley National Laboratory, Berkeley, California 94720, USA*
[3]*Institut Jean Lamour, CNRS–Université de Nancy–UPV-Metz, 54506 Vandoeuvre les Nancy, France*
[4]*Synchrotron SOLEIL, L'Orme des Merisiers, Saint-Aubin, 91192 Gif sur Yvette, France*
[5]*UR1 CNRS/Synchrotron SOLEIL, Saint-Aubin, 91192 Gif sur Yvette, France*
[6]*Commissariatà l'Energie Atomique, SIMA, DSM-IRAMIS-SPCSI, Saclay, 91191 Gif sur Yvette, France*
[7]*Département de Physique, Université de Paris-Sud, 91405 Orsay, France*
[8]*Department of Physics, University of California-Davis, California 95616-8677, USA*
[9]*CNRS/Institut Néel, BP166, 38042 Grenoble, France*

(Received 29 July 2009; published 24 November 2009)

Angle-resolved photoemission and x-ray diffraction experiments show that multilayer epitaxial graphene grown on the SiC(000$\bar{1}$) surface is a new form of carbon that is composed of effectively isolated graphene sheets. The unique rotational stacking of these films causes adjacent graphene layers to electronically decouple leading to a set of nearly independent linearly dispersing bands (Dirac cones) at the graphene K point. Each cone corresponds to an individual macroscale graphene sheet in a multilayer stack where AB-stacked sheets can be considered as low density faults.

In an ideal graphene sheet (near the Dirac point, E_D) the π and π^* bands disperse linearly $E(\Delta k) = \hbar v_F \Delta k$, where v_F is the Fermi velocity and Δk is the momentum relative to the K points of the hexagonal reciprocal unit cell [1]. The two-dimensional dispersion is isotropic and defines a cone with an apex at E_D [1]. For undoped graphene the Fermi energy E_F coincides with E_D so that the Fermi surface consists of six points [see Fig. 1(a)]. This specific electronic structure of graphene is relevant for graphene based electronics for several reasons. For example, electronic energies above (or below) E_D of the order of $\sim$1 eV correspond to wavelengths of order $\sim$1 nm. Consequently, quantum confinement energies in nanoscopic graphene structures will be of the order of $\sim$1 eV, which is considerably greater than the thermal energy at 300 K [2]. This graphene property is essential for room temperature graphene nanoelectronics.

Epitaxial graphene (EG) grown directly on both the SiC(0001) Si face and (000$\bar{1}$) C face has exceptional film quality [3,4]. It is atomically flat and the EG sheets are continuous over macroscopic distances (if not the entire crystal surface). In Si-face few layer EG films, substrate interactions cause charge doping, significant electron-phonon coupling, and distortions in the linear dispersion of the first graphene layer near E_D [5–7]. These are similar to the more substantial substrate induced distortions observed in exfoliated graphene [8,9]. Beyond the first graphene layer, the graphitic AB stacking of few layer Si-face graphene causes the band structure to converge to graphite when the number of layers becomes large [6,10].

In contrast to other forms of graphene, multilayer epitaxial graphene (MEG) grown on the C face of SiC exhibits all the transport properties of an isolated graphene sheet [11–17]. Moreover, Landau level spectroscopy from C-face films has demonstrated unprecedented graphene properties including exceptionally high room temperature mobilities (>200 000 cm^2/V s) and resolved Landau levels in magnetic fields as low as 40 mT [17]. MEG has been shown to have a unique crystal structure. Rather than AB stacked like graphite, MEG films have successive layers that are typically rotated by angles other than the 60° rotation of graphite. This rotational stacking has been theoretically predicted to cause the layers to electronically decouple [18–20].

Here we provide direct experimental evidence for this effect using angle-resolved photoemission spectroscopy (ARPES). In particular we show that the electronic band structure of the individual graphene layers in the MEG stack indeed are essentially unperturbed Dirac cones as expected for isolated graphene sheets. We further show that these films have exceptionally long electron relaxation times and a remarkable absence of distortions in the Dirac cone. The measurements experimentally confirm that the electronic structure of each individual sheet in MEG is essentially that of an isolated graphene sheet as predicted [18–20] and indicated in prior experiments [11–17]. Our results clearly demonstrate that a quasiperiodic (not random) rotational stacking order is responsible for MEG's exquisite 2D properties.

The substrates used in these studies were both n-doped $n = 2 \times 10^{18}$ cm^{-2} 6H and insulating 4H SiC. The graphene layers were grown in a closed rf induction furnace at a temperature of 1550 °C (see Ref. [3] for details). The graphene film thicknesses ranged from 11–12 layers as

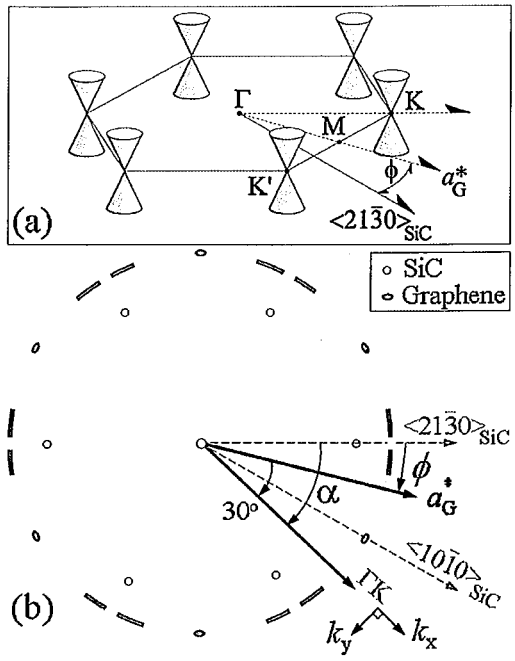

FIG. 1 (color online). (a) 2D Brillouin zone of graphene near E_F showing the six Dirac cones. The graphene reciprocal lattice vector a_G^* (and therefore the cones) are shown rotated by ϕ relative to the SiC $\langle 21\bar{3}0\rangle$ direction. (b) A schematic diffraction pattern of graphene grown on SiC(000$\bar{1}$). The SiC (○) and the graphene patterns (●) from a $\phi = 30°$ rotated film are shown. Diffuse graphene arcs also seen on C face are centered at $\phi = 0°$.

determined by ellipsometry [3]. Graphitized samples were transported in air and thermally annealed at 800–1100 °C in UHV prior to measurement. The furnace-grown MEG samples have exceptionally large sizes. In fact, STM studies have not yet found a single example of a discontinuous top layer in a MEG sample, indicating that at least the topmost layer is a continuous graphene sheet spanning the entire macroscopic surface. Recent STM studies have demonstrated the spectacular structural and electronic properties of the topmost layer [17]. (Note that in contrast, graphene grown in UHV has sheets that are ~50–100 nm in size [3,21,22].)

ARPES measurements were made on different samples at both the Cassiopée beam line at the SOLEIL synchrotron in Gif sur Yvette and at the 12.0.1 beam line at the Advanced Light Source (ALS) at Lawrence Berkeley National Lab with base pressures $<10^{-10}$ Torr. The high-resolution Cassiopée beam line is equipped with a modified Peterson PGM monochromator with a resolution $E/\Delta E \simeq 70\,000$ at 100 eV and 25 000 for lower energies. The detector is a ±15° acceptance Scienta R4000 detector with a base resolution of $\Delta E < 1$ meV (for signal-to-noise concerns the experimental resolution was set at 7 meV). The high-resolution ARPES at the ALS were taken with a total energy resolution of 25 meV using an SES100 electron spectrometer. The surface x-ray diffraction (SXRD) experiments were performed at the Advanced Photon Source, Argonne National Laboratory, on the 6IDB-μCAT UHV beam line with $\hbar\omega = 16.2$ keV.

The primary result of this work is shown in Fig. 2(a), where we display the band structure of an 11-layer graphene film grown on the C face of 6H SiC. Data are taken near the K point ($k_x = 1.704$ Å^{-1}, $k_z \sim 0.02c^*$, where $c^* = 2\pi/6.674$ Å $= 0.941$ Å^{-1}) and not at the H point of graphite ($k_z \sim 0.5c^*$). The figure shows two bright intersecting Dirac cones; a third faint cone is more easily visible in the momentum dispersion curve (MDC) in Fig. 2(b). The Dirac cones in Fig. 2(a) are the first measured nearly unperturbed π bands expected from an isolated graphene sheet. Band maps on different samples and different parts of the sample show similar results: multiple rotated linearly dispersing Dirac cones. Because ARPES is sensitive to 3–4 surface layers at 30 eV, there is no influence on the measured bands from the graphene-SiC interface. The difference $E_D - E_F$ from the graphene surface layers varied from sample to sample. The doping was measured to be as high as ~33 meV p-doped on some samples and n-doped as low as −14 meV on others. This gives a charge density that ranges between $\sim 10^{11}$ and 10^{10} cm^{-2}, comparable to IR measurements from similar films (5×10^9 cm^{-2}) [11]. The doping fluctuation is most likely due to surface adsorbates at these low sample temperatures.

Two points must be stressed. First, these films are *not* graphitic. While the band splitting from AB stacking, seen in bilayer or multilayer graphene films grown on the Si face of SiC, is observed, they are a fraction of the measured cones [5,6,23]. In fact, AB planes are so few they can be viewed as stacking faults in these films. The second point that must be kept in mind is that furnace-grown and UHV-grown graphene are very different, both structurally and electronically. In addition to the poor structural order of UHV-grown graphene, ARPES measurements on UHV-grown C-face graphene show a large electron doping of $E_D - E_F = 0.2$ eV with poorly developed π and σ bands [24]. The doping level difference is likely due to charge coupling between the SiC and the thinner UHV films, while the broad π bands are due to film disorder. The remarkable result of multiple linear bands characteristic of rotated but isolated single graphene sheets confirms predictions that the unique stacking of MEG films grown on the C face of SiC preserves the symmetry of isolated graphene [18–20]. To demonstrate this we first point out a few structural details of C-face films.

We have plotted SXRD azimuthal scans near $\phi = 0°$ and 30° in Fig. 3. Note that, while the exact distribution of graphene rotation angles is sample dependent, the probability of rotation angles near $\phi = 30°$ is nearly equal to the probability of angles near 0°, regardless of sample or film thickness (i.e., the area under the x-ray curves is nearly equal: $\int I_0 d\phi / \int I_{30} d\phi \sim 1.1 \pm 0.3$). This, along with SXRD reflectivity measurements, implies that approximately every other sheet is rotated ~30° instead of the

graphitic 60° [3,20]. This is not the "occasional" small angle rotations proposed by STM measurements [25]. The distribution of rotation angles is determined by an entropy term that selects from a number of SiC-graphene commensurate angles with small energy differences [3]. There are more commensurate angles per radian of arc at $\phi = 0°$, which explains the observed broader distribution in Fig. 3(a) [3]. Also note that the angular width of each discrete rotation is very narrow ($\Delta\phi = 0.045°$) [see the inset in Fig. 3(a)], corresponding to a distance of ~ 1 μm. The rotational domains are smaller than the macroscopic graphene for two reasons. First, the x-ray coherence is limited by the distance between SiC steps (~ 1 μm for these samples). Second, as graphene flows over steps or pleats in the film, small rotations are introduced in the continuous sheet.

To show the correlation between graphene rotation angle ϕ and the ΓK rotation direction α, note that the ΓK direction in ARPES is rotated 30° from the graphene reciprocal space direction, a_G^* [see Fig. 1(a)]. This means that the ΓK direction for a graphene sheet rotated ϕ from the SiC $\langle 21\bar{3}0\rangle$ direction is at an angle $\alpha = \phi + 30°$ (see Fig. 1). We have marked (in red solid lines) the discrete rotation angles of the ARPES Dirac cones (near $\alpha = 30°$) against the angular distribution measured by SXRD in Fig. 3(a) [$\alpha = 30° + \tan^{-1}(k_y/k_{\Gamma K})$, where k_y is taken from ARPES scans like the one shown in Fig. 2]. It is clear that the rotated cones correlate well with the data with many more rotations between 2° and 10°. Note that the SXRD beam size is ~ 3 mm while the ARPES beam size is ~ 40 μm; this is why ARPES sees a small number of discrete rotated cones and SXRD shows a more continuous distribution averaged over a large beam footprint. In the $\alpha = 0°$ azimuth, discrete cones are not resolved [see inset in Fig. 3(b)]. The reason discrete cones are not observed is a combination of the narrow distribution of commensurate rotations at $\phi = 30°$ [note that angular scale in Fig. 3(b) is expanded by a factor of 2 compared to 3(a)] and the wide angular acceptance used for this ARPES data set. Nonetheless, the ARPES distribution of cones again coincides with the SXRD angular distribution [Fig. 3(b)].

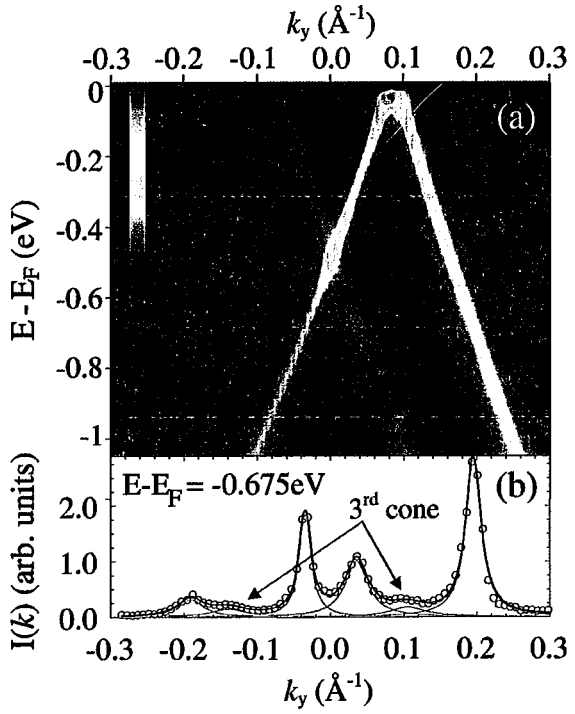

FIG. 2 (color online). (a) ARPES measured band structure of an 11-layer C-face graphene film grown on the 6H SiC. The ARPES resolution was set at 7 meV at $\hbar\omega = 30$ eV. The sample temperature is 6 K. The scan in k_y is perpendicular to the SiC $\langle 10\bar{1}0\rangle_{SiC}$ direction at the K point (see Fig. 1). Two linear Dirac cones are visible. (b) A MDC at $BE = E_F - 0.675$ eV shows a third faint cone. Heavy solid line is a fit to the sum of six Lorentzians (thin solid lines).

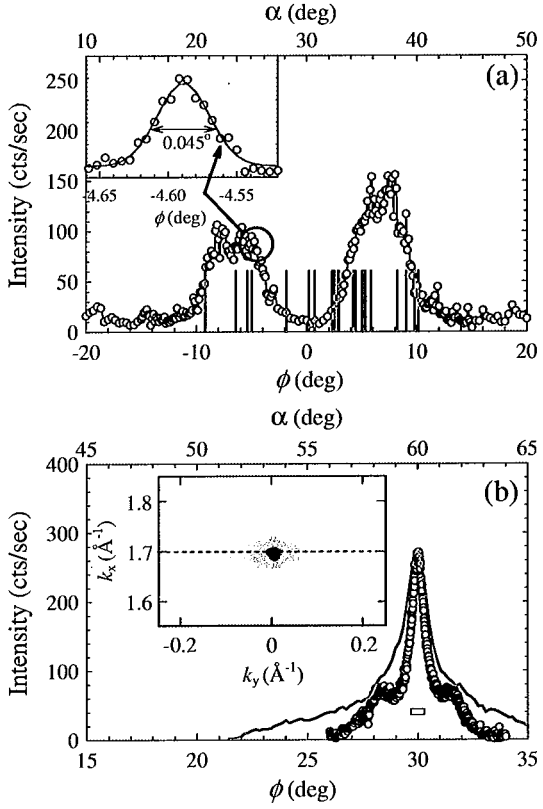

FIG. 3 (color online). (a) SXRD angular distribution of the diffuse arcs around $\phi \sim 0$. Inset in (a) shows a magnified view of a single rotation angle. Vertical red lines mark the angular position α (upper scale) of measured ARPES Dirac cones relative to the $\langle 21\bar{3}0\rangle$ direction. (b) SXRD angular distribution near $\phi \sim 30°$. Inset in (b) is constant energy cut at the Dirac point showing the distribution of cones. Solid red line in (b) is the measured distribution of Dirac cones versus α (upper scale). Rectangle in (b) shows the ARPES angular resolution ($\sim 0.34°$ for this data). ARPES data in (b) was taken at 15 K with $\hbar\omega = 50$ eV.

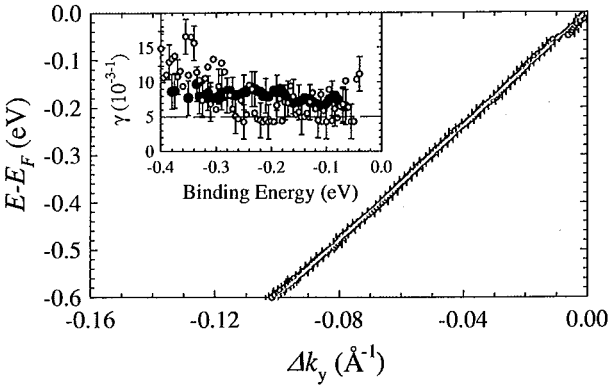

FIG. 4 (color online). $E - E_F$ vs $\Delta k_y = k_D - k_y$. k_y is the Lorentzian center from fits to ARPES MDCs and k_D is the position of the Dirac cone center. Solid line is a linear fit. Inset is a plot of the MDC HWHM γ as a function of binding energy at 6 K (●) and 300 K (○). Data were taken with an energy and k resolution of $\Delta E = 7$ meV and $\Delta k_y \sim 0.01$ Å^{-1} at $\hbar\omega = 30$ eV. Dashed line in the inset is the ARPES resolution used for this data set.

Using high energy and k resolution dispersion curves allows us to measure two important effects. First, the bands are linear. This is demonstrated more clearly in Fig. 4 where we plot the position of one branch of a Dirac cone (determined by fitting the ARPES MDCs to Lorentzian peaks). Within the error bars of the experiment, there are no significant deviations from linearity. The average Fermi velocity, derived from the slope of $E(\Delta k)$, was found to be $\langle v_F \rangle = 1.0 \pm 0.05 \times 10^6$ m/sec for energies down to ~0.5 eV below E_D. This value is larger than v_F for bulk graphite ($v_F \simeq 0.86 \times 10^6$ m/sec) [26] but within error bars of values obtained from both IR measurements ($1.02 \pm 0.01 \times 10^6$ m/s) [11] and scanning tunneling spectroscopy ($1.07 \pm 0.01 \times 10^6$ m/s) [17].

The second point to note is the narrow Lorentzian half width at half maximum (γ) of a MDC [inset of Fig. 4]. γ is inversely proportional to the carrier scattering time $\tau = 1/(2\gamma v_F)$ [27]. Because γ is within error bars of the instrument resolution, we are only able to place a lower bound of $\tau > 20$ fs. This is consistent with τ from IR measurements (100–300 fs) [11]. Also note that there is no measurable change in τ between 6 and 300 K.

ARPES measurements show that the band structure of MEG graphene grown on the C face of SiC consists of multiple undistorted, linearly dispersing graphene bands originating from individual rotated layers in the multilayer film. The observed Dirac cones definitively demonstrate that most of the graphene sheets in the MEG films can be considered as electronically ideal isolated graphene sheets. The origin of this unique behavior is a result of MEG's unique stacking order. All that is required to preserve graphene's linear dispersion in a multilayer stack is to break the AB-stacking symmetry of graphite. This is realized by introducing a relative rotation angle between two adjacent sheets that is not 60° (i.e., graphite stacking) [18–20]. As C-face graphene films grow, the substrate apparently forces relative rotation of ~30 ± 7° making graphitic AB-stacked pairs low density faults in the film. The significance of this result is that uniform single- or double-layer graphene films are not necessarily a requirement for graphene electronics, since even multilayer films have the required electronic properties.

This research was supported by the W. M. Keck Foundation, the Partner University Fund from the French Embassy and the NSF under Grant No. DMR-0820382, and the ANR Foundation (France). The μCAT beam line is supported by the U.S. DOE through Ames Lab under Contract No. W-7405-Eng-82. ARPES measurements at UC Berkeley and LBNL were supported by the DMS and Engineering of the U.S. DOE under Contract No. DEAC03-76SF00098. Both the ALS and APS are operated by the DOE's Office of BES.

This work was supported by the U.S. Department of Energy under Contract No. DE-AC02-05CH11231.

[1] P. R. Wallace, Phys. Rev. **71**, 622 (1947); J. W. McClure, Phys. Rev. **108**, 612 (1957).
[2] C. Berger *et al.*, J. Phys. Chem. B **108**, 19912 (2004).
[3] J. Hass, W. A. de Heer, and E. H. Conrad, J. Phys. Condens. Matter **20**, 323202 (2008).
[4] K. V. Emtsev *et al.*, Nature Mater. **8**, 203 (2009).
[5] S. Y. Zhou *et al.*, Nature Mater. **6**, 770 (2007).
[6] T. Ohta *et al.*, Phys. Rev. Lett. **98**, 206802 (2007).
[7] A. Bostwick, T. Ohta, T. Seyller, K. Horn, and E. Rotenberg, Nature Phys. **3**, 36 (2007).
[8] J. Martin *et al.*, Nature Phys. **4**, 144 (2008).
[9] K. R. Knox *et al.*, Phys. Rev. B **78**, 201408(R) (2008).
[10] C. Riedl, A. A. Zakharov, and U. Starke, Appl. Phys. Lett. **93**, 033106 (2008).
[11] M. Orlita *et al.*, Phys. Rev. Lett. **101**, 267601 (2008).
[12] C. Berger *et al.*, Science **312**, 1191 (2006).
[13] M. L. Sadowski *et al.*, Phys. Rev. Lett. **97**, 266405 (2006).
[14] M. L. Sadowski, G. Martinez, M. Potemski, C. Berger, and W. A. de Heer, Solid State Commun. **143**, 123 (2007).
[15] X. Wu, X. Li, Z. Song, C. Berger, and W. A. de Heer, Phys. Rev. Lett. **98**, 136801 (2007).
[16] W. A. de Heer *et al.*, Solid State Commun. **143**, 92 (2007).
[17] D. L. Miller *et al.*, Science **324**, 924 (2009).
[18] J. M. B. Lopes dos Santos, N. M. R. Peres, and A. H. Castro Neto, Phys. Rev. Lett. **99**, 256802 (2007).
[19] S. Latil, V. Meunier, and L. Henrard, Phys. Rev. B **76**, 201402(R) (2007).
[20] J. Hass *et al.*, Phys. Rev. Lett. **100**, 125504 (2008).
[21] F. Hiebel *et al.*, Phys. Rev. B **78**, 153412 (2008).
[22] G. M. Rutter, J. N. Crain, N. P. Guisinger, T. Li, P. N. First, and J. A. Stroscio, Science **317**, 219 (2007).
[23] S. Y. Zhou *et al.*, Nature Phys. **2**, 595 (2006).
[24] K. V. Emtsev, F. Speck, Th. Seyller, L. Ley, and J. D. Riley, Phys. Rev. B **77**, 155303 (2008).
[25] L. B. Biedermann *et al.*, Phys. Rev. B **79**, 125411 (2009).
[26] Yu. A. Bychkov and G. Martinez, Phys. Rev. B **77**, 125417 (2008).
[27] M. Calandra and F. Mauri, Phys. Rev. B **76**, 205411 (2007).

DISCLAIMER